Wavelet transform method
of phase-step determination

YEU-JENT HU[1], JIN-YI SHEU[1], JIUNN-CHYI LEE[1], YA-FEN WU[2*]

[1]Department of Electrical Engineering, Taipei Chengshih University of Science and Technology,
 Taipei, 112 Taiwan

[2]Department of Electronic Engineering, Ming Chi University of Technology,
 New Taipei City, 243 Taiwan

*Corresponding author: yfwu@mail.mcut.edu.tw

The phase-shifting technique is the most popular phase-retrieving technique applied in optical testing. Most of the phase retrieval algorithms rely on stability and accuracy of phase steps. A sufficiently exact phase-step calibration is necessary for phase measurements with high accuracy. We introduce a new method for phase-step calibration between interferograms. The method is based on a recently introduced continuous wavelet transform demodulation technique. For the method proposed here only two phase-stepped images are required. Simulation results indicate that the phase shift error of the proposed method is less than 0.05%.

Keywords: continuous wavelet transform, interferometry, phase measurement, fringe pattern.

1. Introduction

The phase-shifting interferometry (PSI) is the most popular phase-retrieving technique applied in optical testing. In PSI, most of the phase retrieval algorithms rely on the stability and accuracy of the phase steps. Phase-shifter miscalibration is a major source of systematic error that limits the phase measurement accuracy. Therefore, a sufficiently exact phase-step calibration is a necessary and important task in phase measurements with high accuracy. Many calibration techniques [1–5] have been developed to measure an unknown phase step. In the techniques using the Carré algorithm [6] four phase-stepped images are required. This algorithm was constructed not only to obtain the phase step but also to obtain information on all four unknown quantities, *i.e.*, the background intensity, the modulation, the phase step, and, most important, the phase to be measured. The assumption in the Carré approach is that the phase step δ, the background intensity I_b, and the modulation depth M are constant for all recordings.

In recent years, the wavelet transform (WT) was found to be applicable to different tasks, such as pattern recognition, image compression and sound analysis [7, 8].

Continuous wavelet transform (CWT) was also used for phase extraction on different types of fringe patterns with spatial carrier [9, 10]. The WT is an important linear time-frequency (space-frequency) representation, which can represent a signal by its localization both in the time space and frequency planes [11–13].

In this study, continuous wavelet transform is applied to extract the phase-step from two fringe patterns. The phase-step calibration can be obtained by extracting the ridge of the wavelet coefficients. The principle of the method proposed is demonstrated by simulation of phase demodulation of fringe pattern using CWT technique. In Section 2, we introduce a continuous wavelet transform and discuss the space-frequency localization properties of wavelets. A new CWT demodulation technique is described in this section, where the phase-step between two images can be obtained from the wavelet ridge. In Section 3, the CWT method is applied to phase-step calibration, where results of the simulations are presented. The conclusions are discussed in Section 4.

2. Phase-step calibration by wavelet transform

The wavelet transform has become an effective tool in many research areas, for example, being a useful mathematical tool, it can be employed in this application. The CWT of a signal $f(x)$ is defined as its inner product with a family of wavelet functions $\psi_{a,b}(x)$ [14, 15]

$$W_f(a, b) = \int_{-\infty}^{\infty} f(x)\, \psi_{a,b}^*(x)\, \mathrm{d}x \tag{1}$$

$$\psi_{a,b}(x) = \frac{1}{\sqrt{a}}\, \psi\left(\frac{x-b}{a}\right), \quad b \in R, \quad a > 0 \tag{2}$$

where $\psi(x)$ is the mother wavelet, $\psi_{a,b}(x)$ is a set of basis functions, called daughter wavelet and obtained from the mother wavelet, a is the scaling parameter related to the frequency, b is the translation parameter, and asterisk denotes a complex conjugate. The factor $1/\sqrt{a}$ in Eq. (2) is used to keep the energy of $\psi_{a,b}(x)$ constant during dilation and translation. In this study, the wavelet ridge is applied to determine the phase step between two fringe patterns. To illustrate the properties of the ridge, the Morlet wavelet is chosen as mother wavelet because it gives a better resolution in spatial and frequency domains. The Morlet wavelet can be written as [13]

$$\psi(x) = g(x)\exp(i\eta x) \tag{3}$$

where μ is the mother frequency, $g(x)$ is a symmetric window function this is, generally, a Gaussian function as it provides the smallest Heisenberg box. Suppose that the intensity distribution of the two images $I_0(x, y)$ and $I(x, y)$ can be expressed as

$$I_0(x, y) = A_0 + B_0 \cos\left[\psi(x, y)\right] \tag{4}$$

$$I(x, y) = A + B \cos\left[\psi(x, y) + \delta\right] \tag{5}$$

where A and A_0 are the background intensities, B and B_0 are the modulation intensities, $\psi(x, y)$ is the phase of the image $I_0(x, y)$, and δ is the phase step.

For clarity, let $I_0(x)$ and $I(x)$ represent a row of the fringe patterns $I_0(x, y)$ and $I(x, y)$, respectively. The wavelet transforms of $I_0(x)$ and $I(x)$ on the ridge are then given by [14]

$$W_I(a_m, b) = \frac{\sqrt{a_m}}{2} B \exp\left\{i\left[\psi(b) + \delta\right]\right\} \hat{g}(0) \tag{6}$$

$$W_{I_0}(a_{0m}, b) = \frac{\sqrt{a_{0m}}}{2} B_0 \exp\left\{i\left[\psi(b)\right]\right\} \hat{g}(0) \tag{7}$$

From Eqs. (6) and (7), the phase step is calculated by

$$\delta = \text{Im}\left\{\ln\left[W_I(a_m, b)\right]\right\} - \text{Im}\left\{\ln\left[W_{I_0}(a_{0m}, b)\right]\right\} \tag{8}$$

where $\text{Im}\{\ln[W_I(a_m, b)]\}$ denotes the imaginary part of the wavelet transform of $I(x)$, a_m denotes the value of a at instant b on the ridge.

3. Computer simulation

For the method proposed here only two phase-stepped images are required. To test the method described above, we created two fringe patterns that can be written as

$$I_0(x, y) = A_0 + B_0 \cos\left[2\pi\psi(x, y)\right] + n(x, y) \tag{9}$$

$$I(x, y) = A + B \cos\left[2\pi\psi(x, y) + \delta\right] + n(x, y) \tag{10}$$

where $\psi(x, y) = 0.55(x^2 + y^2)^2 + 1.5y(x^2 + y^2) + 0.5(x^2 + 3y^2) + 1.2(x^2 + y^2) + 8x$.

The global phase shift between the two interferograms is 1.0472 rad, $n(x, y)$ is random noise, the noise mean and variance are preset at 0 and 0.14, the data are uniformly sampled 129×129 points in the unit square, which are shown in Fig. 1. Figures 2**a** and 2**b** represent the one-dimensional signals of the row 50 of Figs. 1**a** and 1**b**, respectively.
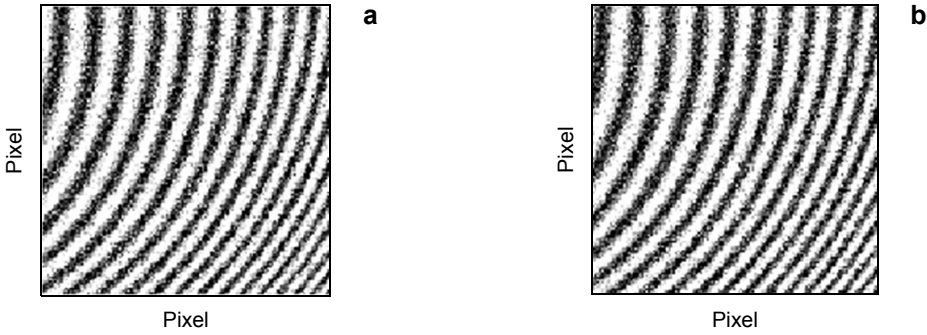
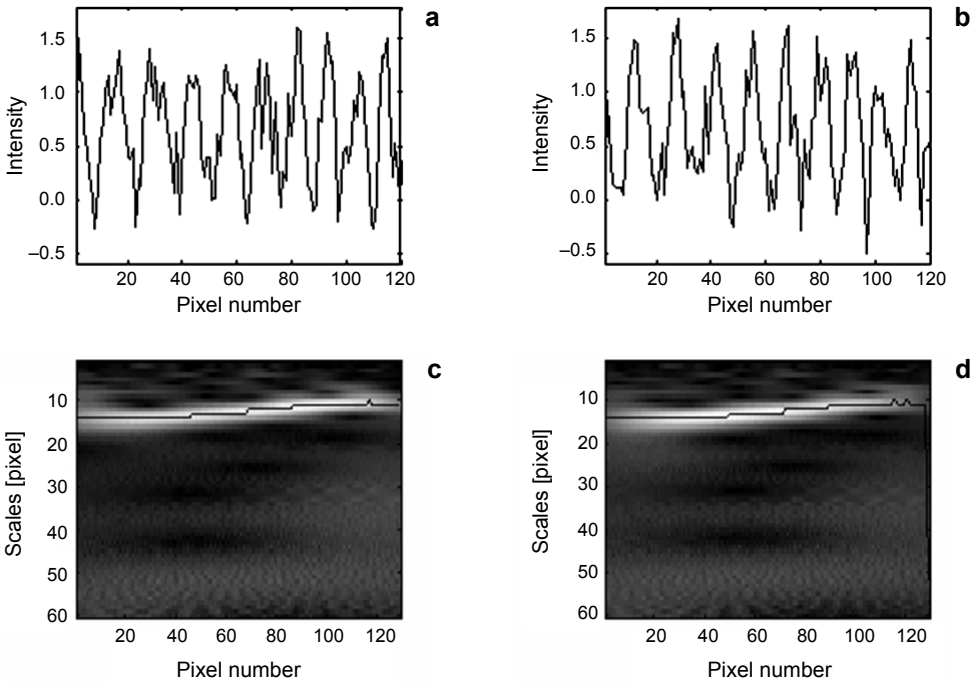Fig. 1. Simulated interferograms with phase-step value of 0 (**a**), and 1.0472 rad (**b**).

Fig. 2. The one-dimensional signals of the row 50 of Fig. 1**a** (**a**), and Fig. 1**b** (**b**); modulus of the CWT and corresponding ridge of Fig. 2**a** (**c**), and modulus of the CWT and corresponding ridge of Fig. 2**b** (**d**).

Processed by CWT technique in the above case, Figs. 2**c** and 2**d** show the modulus of CWT coefficient of Figs. 2**a** and 2**b**, respectively. The solid curve shows the ridge where the maximum modulus is formed. The maximum modulus value is determined by computing the maximum correlation coefficients of the original signal and daughter wavelets, which reflect similarity between the wavelet and load signal. To avoid
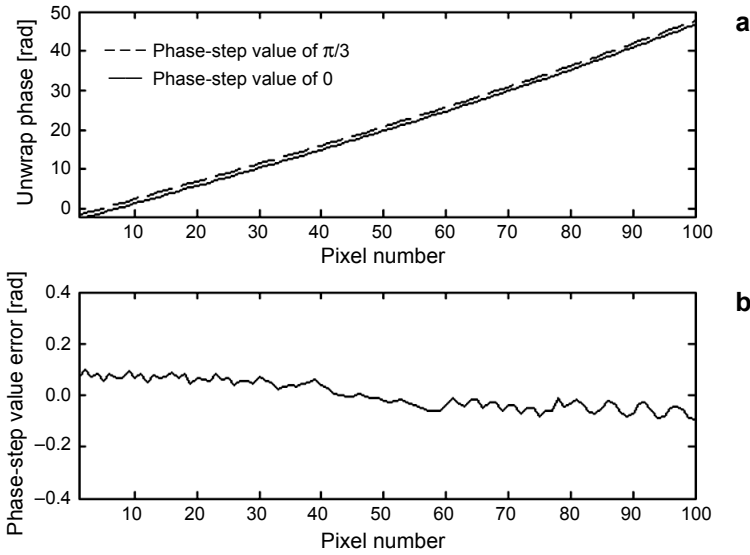
Fig. 3. Phase error analysis by CWT algorithm: calculated phase distribution (**a**), and phase-step value error (**b**).

the inherent edge distortion error of the CWT, we ignore 20 pixels at the boundary. From Eqs. (6) and (7), the unwrapped phase can be retrieved, which is shown in Fig. 3**a**. A very accurate estimation of δ can be obtained if we calculate the phase-step for each row and finally average the values obtained from each row. The phase-step value error can be estimated, which is shown in Fig. 3**b**.

The phase-step calibration results are summarized in the Table and shown in Fig. 4. Before the noise was added, the phase-step estimated by the new algorithm had shown high accuracy. After the noise was introduced, it was found that the error in the obtained

T a b l e. Phase-step calibration results.

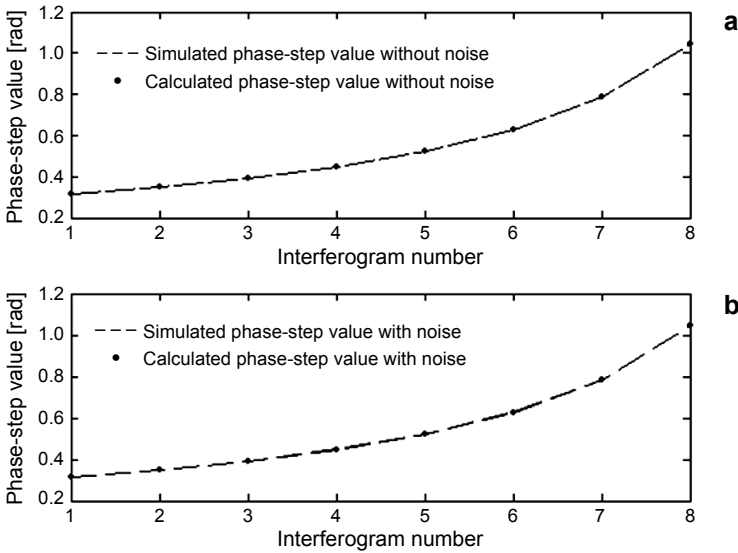| Simulated phase step value [rad]	Calibration result without noise [rad]	Error [%]	Calibration result with noise [rad]	Error [%]
0.3142	0.3141	−0.039	0.3128	−0.34
0.3491	0.3490	−0.045	0.3476	−0.41
0.3927	0.3926	−0.040	0.3910	−0.44
0.4488	0.4485	−0.037	0.4469	−0.42
0.5236	0.5235	−0.025	0.5222	−0.27
0.6283	0.6280	−0.028	0.6259	−0.38
0.7854	0.7850	−0.021	0.7837	−0.22
1.0472	1.0470	−0.019	1.0456	−0.15

Fig. 4. Calibration curve for the phase-step: without added noise (**a**), and with added noise (**b**).

phase step was less than 0.5%. It can be seen that the simulated results agree well with theoretical ones.

4. Conclusions

The phase step calibration algorithm described in this paper allows an arbitrary phase step to be calibrated between two interferograms. We have proposed a simple method for phase-shift measurement between two interferograms. The main feature of the method proposed is to determine accurate phase-step values from two fringe patterns using wavelet coefficients along the wavelet ridge. Compared with the traditional methods used for the same purpose, our method has the advantages of high accuracy and high antinoise ability. We believe that it may find practical applications in related fields, especially in phase-shifting interferometry, for elimination of the phase-shift error. The wavelet transform method proposed in this paper has demonstrated the validity of the new phase-step calibration method.

References

[1] CHENG Y.Y., WYANT J.C., *Phase shifter calibration in phase-shifting interferometry*, Applied Optics **24**(18), 1985, pp. 3049–3052.
[2] JAMBUNATHAN K., WANG L.S., DOBBINS B.N., HE S.P., *Semi-automatic phase shift calibration using digital speckle pattern interferometry*, Optics and Laser Technology **27**(3), 1995, pp. 145–151.
[3] VAN BRUG H., *Phase-step calibration for phase-stepped interferometry*, Applied Optics **38**(16), 1999, pp. 3549–3555.
[4] CHEN X., GRAMAGLIA M., YEAZELL J.A., *Phase-shift calibration algorithm for phase-shifting interferometry*, Journal of the Optical Society of America A **17**(11), 2000, pp. 2061–2066.

[5] GOLDBERG K.A., BOKOR J., *Fourier-transform method of phase-shift determination*, Applied Optics **40**(17), 2001, pp. 2886–2894.

[6] MALACARA D., *Optical Shop Testing, in Pure and Applied Optics*, Wiley, 1992.

[7] FREYSZ E., POULIGNY B., ARGOUL F., ARNEODO A., *Optical wavelet transform of fractal aggregates*, Physical Review Letters **64**(7), 1990, pp. 745–748.

[8] KRONLAND-MARTINET R., MORLET J., GROSSMANN A., *Analysis of sound patterns through wavelet transforms*, International Journal of Pattern Recognition and Artificial Intelligence **1**(2), 1987, pp. 273–302.

[9] WATKINS L.R., TAN S.M., BARNES T.H., *Determination of interferometer phase distributions by use of wavelets*, Optics Letters **24**(13), 1999, pp. 905–907.

[10] FANG J., XIONG C.Y., YANG Z.L., *Digital transform processing of carrier fringe patterns from speckle-shearing interferometry*, Journal of Modern Optics **48**(3), 2001, pp. 507–520.

[11] COMBES J.M., GROSSMANN A., TCHAMITCHIAN P., *Wavelets: Time-Frequency Methods and Phase Space*, Springer, 1989.

[12] MALLAT S.G., *A theory for multiresolution signal decomposition: The wavelet representation*, IEEE Transactions on Pattern Analysis and Machine Intelligence **11**(7), 1989, pp. 674–693.

[13] DAUBECHIES I., *The wavelet transform, time-frequency localization and signal analysis*, IEEE Transactions on Information Theory **36**(5), 1990, pp. 961–1005.

[14] MALLAT S., *A Wavelet Tour of Signal Processing*, Academic Press, 1999.

[15] DAUBECHIES I., *Ten Lectures on Wavelets*, SIAM, Philadelphia, 1992.